Angular distributions of desorbing N_2 in thermal N_2O decomposition on Rh(100)

Tatsuo Matsushima [1*] and Anton Kokalj [2]

[1] Catalysis Research Center, Hokkaido University, Sapporo, 001-0021 Japan

[2] Jožef Stefan Institute, 1000 Ljubljana, Slovenia

[*] Corresponding author, Fax: +81-11-706-9120, E-mail: tatmatsu@cat.hokudai.ac.jp

(Received; 24 August 2006 ; accepted for publication; January 2007)

Abstract

The angular distribution of desorbing N_2 was studied in the decomposition of N_2O(a) on Rh(100) at 60-140 K by means of angle-resolved temperature-programmed desorption. N_2 desorption shows two peaks at around 80 K and 110 K. At low N_2O coverage, the former collimates far from the surface normal toward the [001] direction, whereas at high coverage, the desorption sharply collimates along the surface normal. The adsorption form of N_2O and its dissociation were also examined by DFT-GGA

calculations. Dissociating N_2O is proposed to be lying along the [001] direction at low coverage and to change to an upright form bonding through the terminal oxygen at high coverage.

Key words; Thermal desorption, Nitrous oxide, Rhodium, Surface chemical reaction, Angle-resolved DIET, Catalysis, Density functional theory calculations.

I. Introduction

The reduction of nitrous oxide on rhodium surfaces has received much attention because of its importance in controlling the catalytic deNOx process. N_2O is not only an undesirable byproduct in the NO reduction on this best catalyst but also the key intermediate in controlling the selectivity toward N_2 [1]. Knowledge of this intermediate is still limited because of the presence of several surface-nitrogen removal pathways in the deNOx process. This paper is the first to deliver the angular distribution of desorbing N_2 in the thermal decomposition of adsorbed N_2O on Rh(100). N_2 desorption shows two peaks at around 80 K (β_2-N_2) and 110 K (β_1-N_2). The former sharply collimates at 66° off normal in the plane along the [001] direction at low N_2O coverage, indicating four-directional desorption, whereas, at high coverage, its desorption shifts along the surface normal. The adsorption form of N_2O and its dissociation were also examined by density-functional theory calculations (DFT) with the generalized gradient approximation (GGA).

The characteristic spatial distribution of desorbing N_2 in the deNOx process is useful to identify the intermediates emitting products. The desorption of N_2 with hyper-thermal energy in the N_2O decomposition is sharply collimated in an inclined way in the plane along the N-N-O bond on Pd(110) and Rh(110), i.e., the parent molecule orientation is preserved in the distribution. On Rh(100), similar inclined N_2 desorption along the [001] direction is observed only at limited N_2O coverage. At high coverage, another N_2O adsorption form is suggested.

II. Technical details

2.1 Experimental

Two UHV apparatuses were used. One has low-energy electron diffraction (LEED) and X-ray photonelectron spectroscopy (XPS) facilities for the survey of surface-cleaning procedures, and the other has three chambers for angle-resolved temperature-programmed desorption (AR-TPD) [2]. The reaction chamber has a mass spectrometer for angle-integrated (AI) desorption analysis as well as a cryo-plate cooled to about 25 K yielding a pumping rate of about 9 m^3/s, which is large enough to prevent the N_2 scattered in the reaction chamber from penetrating the analyzer [3].

A rhodium crystal with (100) planes (1 mm thick with a 9 mm diameter) was rotated to change the desorption angle (polar angle; θ) in the normally directed plane at the crystal azimuth along either the [001] or [011] direction. The LEED pattern showed a sharp (1×1) form after the surface was cleaned by Ar^+ ion bombardments, heating in

5×10^{-8} Torr oxygen at a surface temperature (T_S) of 850 K and then in 6×10^{-8} Torr hydrogen. The crystal was heated in H_2 before every N_2O exposure to remove the surface oxygen [4]. The $^{15}N_2O$ coverage, Θ_{N2O}, was determined from the $^{15}N_2O$ exposure relative to the value to a monolayer. The completion of a monolayer was defined by the appearance of a sharp $^{15}N_2O$ desorption peak from multilayers at 84 K. The density of the monolayer was estimated to be one fourth of the surface rhodium atom density from a comparison with the $^{13}C^{18}O$ desorption [5]. Hereafter, the isotope ^{15}N is described as N in the text. No super-structures were found in LEED observations after N_2O adsorption at 78 K.

2.2 Computational

The calculations were performed in the framework of DFT-GGA [6] using the plane-wave basis set and ultrasoft pseudopotentials [7,8] as implemented in the PWscf code contained in the Quantum ESPRESSO package [9], while molecular graphics were generated using the XCRYSDEN program [10]. The perfect Rh(100) surface was modeled by periodically repeated slabs consisting of five (100) layers and N_2O adsorption was modeled at 1/4 and 1/9 ML coverages using (2×2) and (3×3) supercells respectively. Further computational details are described elsewhere [11]. Transition states and activation energies for N_2O dissociation have been calculated by climbing-image nudged-elastic-band method [12] using the (2×2) supercells.

III. Results

3.1 AR-TPD results

N_2O was introduced at T_S = 50-55 K. N_2O(a) is either desorbed in the subsequent heating or decomposed, emitting N_2 at 60-130 K (Fig. 1a). The N_2O desorption is noticeable above Θ_{N2O} = 0.5 in the range of 100-130 K. The N_2 desorption peaks at 100-120 K (β_1-N_2) and 70-95 K (β_2-N_2). The β_1-N_2 signal above Θ_{N2O} = 0.7 is largely corrected by the N_2O fragmentation in the analyzer. The β_2-N_2 signal shows remarkable enhancement in the surface normal direction. It increases rapidly above Θ_{N2O} = 0.3, whereas the β_1–N_2 signal increases slowly. Below Θ_{N2O} = 0.20, the β_2-N_2 signal is intensified at around 66º off normal toward the [001] direction. The β_2-N_2 signal at this position decreases with increasing N_2O coverage (Fig. 1b). On the other hand, the β_1-N_2 signal increases and its peak shifts to lower temperatures. These comparisons indicate that the angular distribution of β_2-N_2 changes from an inclined form to a normally directed way with increasing N_2O coverage.

The AR-TPD spectra of β_2-N_2 below Θ_{N2O} = 0.15 are intensified at around θ = 68º in the plane along the [001] direction (Fig. 2(a)). In the analysis of the noisy AR signals, the average level was estimated by curve fitting, in which a Gaussian form was assumed [13]. The resultant angular distribution along the [001] direction is sensitive to the coverage (Fig. 2b). The distribution changes from a three-directional form to the normally directed one with increasing N_2O coverage. The inclined desorption component is sharp as approximated in a $\cos^{25}(\theta \pm 66)$ form at Θ_{N2O} = 0.16. The collimation angle slightly shifts to smaller values at higher coverage. The normally directed component was approximated into a $\cos^{7\text{-}8}(\theta)$ form at Θ_{N2O} = 0.68. On the

other hand, in the plane along the [011] direction, the N_2 desorption is sharply directed along the surface normal even at low coverage. The other peak (β_1-N_2) shows a cosine distribution.

3.2 DFT results

Two kinds of adsorption forms of N_2O were characterized by DFT-GGA, i.e., (i) an upright (or slightly tilted—precise estimation of the tilt angle is difficult due to the flatness of the potential energy surface) form with the terminal nitrogen bonding to the surface, and (ii) a lying form attached to the surface with both terminal N and O atoms (Fig. 3). The upright form prefers to adsorb on the top site with an adsorption energy (E_{ads}) of 0.46 eV at 1/9 ML coverage, whereas on the bridge site it is about 0.1 eV smaller. In the lying form, both terminal atoms are bonded to neighboring top sites. The [011]-oriented form (E_{ads}= 0.50 eV at 1/9 ML) is more stable than the [001]-oriented one (E_{ads}= 0.40 eV at 1/9 ML). The adsorption energies at larger 1/4 ML coverage are slightly smaller than at 1/9 ML, the largest difference being 0.05 eV for the lying [011]-oriented form, which is due to close distance between the terminal O and N atoms of neighboring molecules. The upright and lying adsorption forms are very similar to those on Rh(110), but the current adsorption energies are smaller [11]. This is reasonable because the surface metal atoms on (110) surface are less coordinated and thus more reactive. The dissociation to N_2(a)+O(a) proceeds during the geometry optimization of the lying form with both terminal atoms bonded to the adjacent bridge sites. Special attention has been given to the search for either an upright or a tilted form attached through the O atom to the surface because such an

adsorbed structure could be a precursor in the desorption of N_2 along the surface normal. The calculations suggest, however, that N_2O cannot adsorb with its O-atom in an upright (or titled) configuration.

4. Discussion

4.1 Desorption components

N_2O decomposition yields two N_2 desorption peaks at 60-130 K. Because of its cosine distribution, β_1-N_2 is desorbed from adsorbed N_2. Such N_2(a) may be formed either at the adsorption temperature or in the subsequent heating. The desorption from N_2(a) on Rh(100) was reported to take place at around 110 K [14].

At low N_2O coverage, β_2-N_2 appears at lower temperatures. This is due to direct desorption from the N_2O decomposition because of the sharp angular distribution. For highly inclined N_2 desorption, the decomposition of N_2O oriented in the [001] direction was first proposed on Pd(110) (1×1), where desorbing N_2 collimated at 43º off normal [1]. On Rh(110), the N_2 desorption collimates 65-68 º off normal along the [001] direction [2]. The [001]-oriented N_2O as well as the tilted form bonded through the terminal nitrogen was predicted on Rh(110) and Pd(110) by DFT-GGA calculations [13,15]. Both forms were later confirmed on Pd(110) by scanning tunneling microscope and the near-edge X-ray absorption fine structure [16].

According to the DFT-GGA calculations, the [001]-oriented N_2O(a) is bent on Pd(110) and Rh(110) with the terminal nitrogen and oxygen atoms pointing toward the surface. On Rh(100), the bending is enhanced along the [011] direction because of the

shorter nearest-neighbor rhodium atom distance. These lying forms are plausible precursors for the dissociation to release the oxygen. The adsorption heat was estimated to be about 0.28 eV from the desorption peak temperature (ca 110 K). The calculated values (0.4 ~ 0.5 eV) are therefore overestimated. We also estimated activation energies for the dissociation of [001]- and [011]-oriented N_2O, and located the respective transition states (TS). The activation energies are fairly small, about 0.1 eV for both lying [001]- and [011]-oriented forms. Both TS are reactant-like and the reaction coordinate is mainly along the N-O distance, which is elongated by about 0.19 and 0.24 Å at the TS of the [001]- and [011]-oriented forms, respectively. The calculated activation energies, however, are too small to account for the dissociation at around 70 K. The dissociation in the subsequent heating might be retarded by oxygen deposited at the adsorption temperature as observed on Rh(110) [2]. At present, on the basis of DFT-GGA calculations, we are not able to explain why the [001]-oriented N_2O dissociates easily. Possibly the dispersion interactions, which are not treated properly in DFT-GGA, may be important in this context and account for this discrepancy.

4.2 Inclined and normally directed desorption

The sharp inclined N_2 desorption comes from the dissociation of the [001]-oriented N_2O in a similar way to that on Rh(110) and Pd(110). From the surface symmetry of Rh(100), it shows four-directional desorption. This inclined desorption shows a similar collimation angle to that on Rh(110), where the distribution is a form of $\cos^{10}\{\theta - (65\pm4)\}$. There are remarkable differences in their angular distributions, i.e., the co-existence of normally directed desorption and sharper inclined desorption.

No upright (or tilted) N_2O adsorption bonding through the terminal oxygen has been found on clean Pd(110) and Rh(110) surfaces in the DFT-GGA calculations [11,15] and experimentally no normally directed N_2 desorption has been found on these surfaces [2]. However, it is unlikely that the product N_2 is sharply emitted along the surface normal without such an adsorption form because of the lack of an associative process of N(a) in the N_2O dissociation. For the normally directed desorption, the lying form is unlikely to be the precursor.

It should be noted that the inclined component is enhanced at small N_2O coverage and the normally directed desorption is increased above about Θ_{N2O}= 0.20. In other words, the inclined desorption is remarkable on oxygen-free surfaces and the normally directed component takes place in the presence of deposited oxygen. The adsorption form of N_2O may be changed in the presence of oxygen. In fact, the heat of adsorption was reported to increase on Ru(001) by the addition of a small amount of oxygen [17]. In fact, the present experiments show that β_2-N_2 formation is extended to higher temperatures when more oxygen is deposited. Surface rhodium atoms modified by oxygen may be positively charged, yielding adsorption sites for standing N_2O with the terminal oxygen bonding to the surface. Such a form has been proposed on rhodium oxides [18].

Acknowledgements

This work was supported in part by Grant-in-Aid No. 18550114 for General Scientific Research from the Japan Society for the Promotion of Science as well as by a 1996

COE special equipment program of the Ministry of Education, Science, Sports, and Culture of Japan.

References

[1] T. Matsushima, Surf. Sci. Rep. 52 (2003) 1 and there in.

[2] K. Imamura and T. Matsushima, Catal. Lett. 97 (2004) 197.

[3] M. Kobayashi and Y. Tuzi, J. Vac. Sci. Technol. **16** (1979) 685.

[4] G. B. Fisher and S. J. Schmieg, J. Vac. Sci. Technol. A 1 (1983) 1064.

[5] A.P. Van Bavel, M.J.P. Hopstaken, D. Curulla, J.W. Niemantsverdriet, J.J. Lukklen and P. A. Hilbers, J. Chem. Phys. 119 (2003) 524.

[6] J. P. Perdew, K. Burke and M. Ernzerhof, Phys. Rev. Lett. 77 (1996) 3865.

[7] D. Vanderbilt, Phys. Rev. B 41 (1990) 7892.

[8] Ultrasoft pseudopotentials (US PP) for the nitrogen and rhodium atoms were obtained from the PWscf's pseudopotential download page, http://www.pwscf.org/pseudo.htm. Files: N.pbe-rrkjus.UPF, and Rh.pbe-rrkjus.UPF. The pseudopotential for oxygen atom is the one used in the reference: A. Dal Corso, Phys. Rev. B 64 (2001) 235118.

[9] S. Baroni, A. Dal Corso, S. de Gironcoli, P. Giannozzi, C. Cavazzoni, G. Ballabio, S. Scandolo, G. Chiarotti, P. Focher, A. Pasquarello, K. Laasonen, A. Trave, R. Car, N. Marzari and A. Kokalj: Quantum ESPRESSO: Open-Source Package for Research in Electronic Structure, Simulation, and Optimization, http://www.pwscf.org/ (2005).

[10] A. Kokalj: Comput. Mater. Sci. 28 (2003) 155 [Code, http://www.xcrysden.org/ (2005)]

[11] A. Kokalj, T. Matsushima, J. Chem. Phys. 122 (2005) 034708.

[12] G. Henkelman, B. P. Uberuaga, and H. Jonsson, J. Chem. Phys. 113 (2000) 9901.

[13] H. Horino, S. Liu, A. Hiratsuka ,Y. Ohno and T. Matsushima, Chem. Phys. Lett. 341 (2001) 419.

[14] H. A. C. M. Hendrickx, A. Hoek and B. E. Nieuwenhuys, Surf. Sci. 135 (1983) 81.

[15] A. Kokalj, I. Kobal and T. Matsushima, J. Phys. Chem. B 107 (2003) 2741.

[16] K. Watanabe, A. Kokalj, H. Horino, I.I. Rzeznicka, T. Takahashi, N. Nishi and T. Matsushima, Jpn. J. Appl. Phys. 45 (3B) (2006) 2290.

[17] H.H. Huang, C.S. Seet, Z. Zou and G.Q. Xu, Surf. Sci. 356 (1996) 181.

[18] A. L. Yakovlev, G. M. Zhidomirov and R. A. Van Santen, Catal. Lett. 75 (2001) 45.

Figure captions

Fig. 1 AR-TPD spectra of desorbing $^{15}N_2$ from Rh(100) exposed to various amounts of $^{15}N_2O$ at 60 K. The desorption angles θ are (a) 0° and (b) 68° toward the [001] direction. Closed symbols; observed signal of mass/e = 30. Open symbols; signals after fragment correction. The heating rate was 1.5 K/s.

Fig. 2 (a) AR-TPD spectra of $^{15}N_2$ observed at different desorption angles in the plane along the [001] direction. Θ_{N2O} = 0.15. The curves were deconvoluted into two Gaussian peaks for smoothing. (b) Angular distributions of desorbing β_2-$^{15}N_2$ in the plane along the [001] direction at Θ_{N2O} = 0.16, 0.32 and 0.68. The ordinate was normalized to the β_2-N_2 signal at the surface normal direction at Θ_{N2O} = 0.68. The distributions were deconvoluted into two inclined components and a normally directed component, as shown by broken curves. The solid lines indicate their summations. A top view of the surface and its azimuth are shown on the top.

Fig. 3 Top and side views of DFT-GGA optimized N_2O(a) structures on Rh(100) at 1/9 ML. The larger gray balls are Rh atoms, while the smaller red (blue) balls are oxygen (nitrogen) atoms. The corresponding chemisorption energies are also shown.

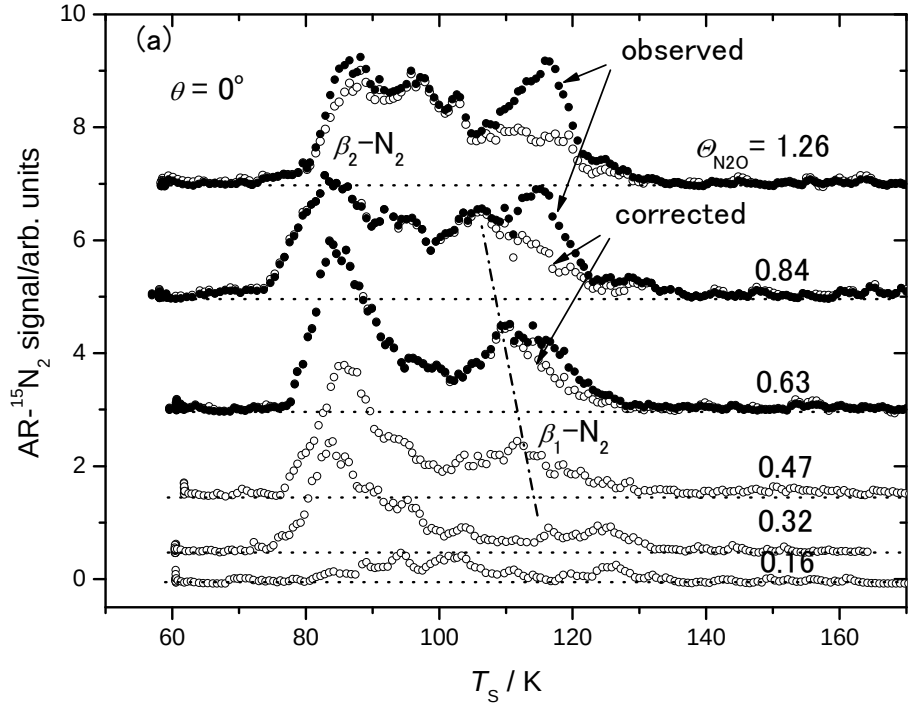
(a)
θ = 0°
observed
corrected
β2–N2
β1–N2
ΘN2O= 1.26
0.84
0.63
0.47
0.32
0.16
AR-15N2 signal/arb. units
TS / K

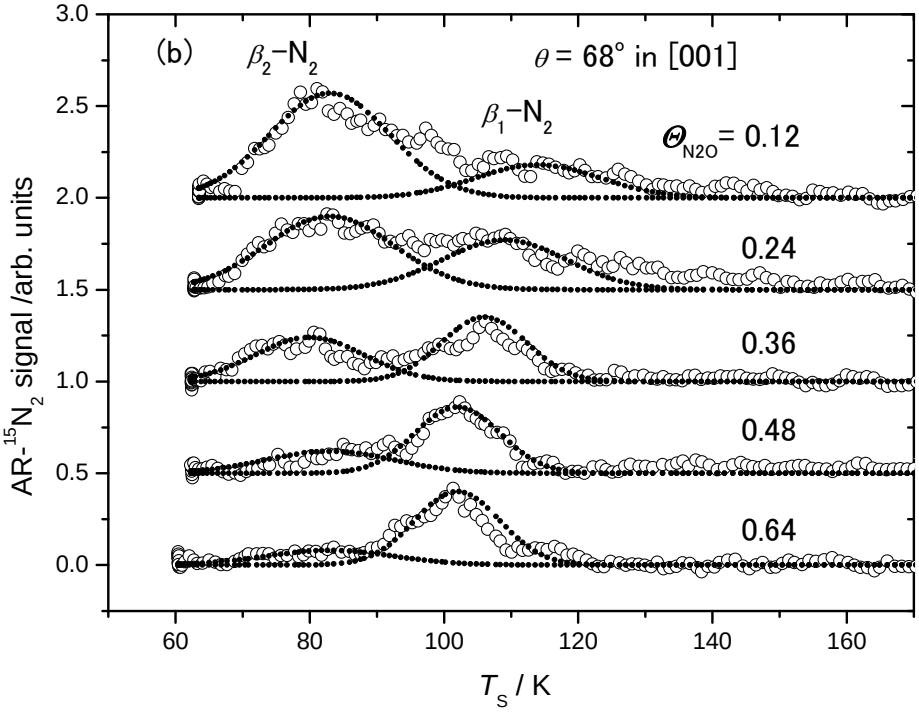
(b)
β2–N2
θ = 68° in [001]
β1–N2
ΘN2O= 0.12
0.24
0.36
0.48
0.64
AR-15N2 signal /arb. units
TS / K

Fig.1 Mat

Fig.2Mat

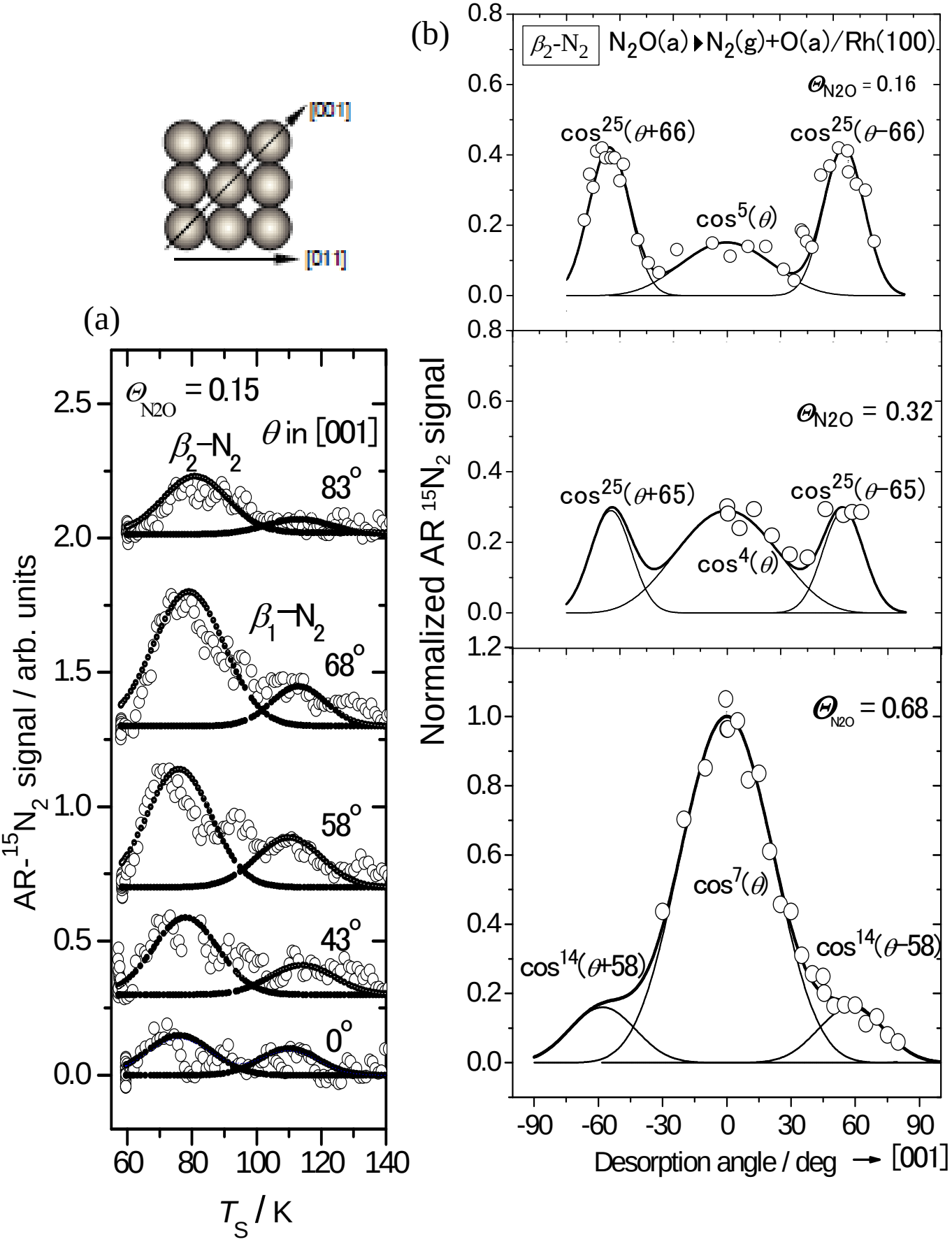
[001]
[011]
(a)
Θ_{N2O} = 0.15
β_2–N_2
θ in [001]
83°
β_1–N_2
68°
58°
43°
0°
AR-$^{15}N_2$ signal / arb. units
T_S / K
(b)
β_2-N_2
$N_2O(a) \blacktriangleright N_2(g)+O(a)/Rh(100)$
Θ_{N2O} = 0.16
$\cos^{25}(\theta+66)$
$\cos^{25}(\theta-66)$
$\cos^{5}(\theta)$
Θ_{N2O} = 0.32
$\cos^{25}(\theta+65)$
$\cos^{25}(\theta-65)$
$\cos^{4}(\theta)$
Θ_{N2O} = 0.68
$\cos^{7}(\theta)$
$\cos^{14}(\theta+58)$
$\cos^{14}(\theta-58)$
Normalized AR $^{15}N_2$ signal
Desorption angle / deg → [001]

(3×3)-N_2O/Rh(100)

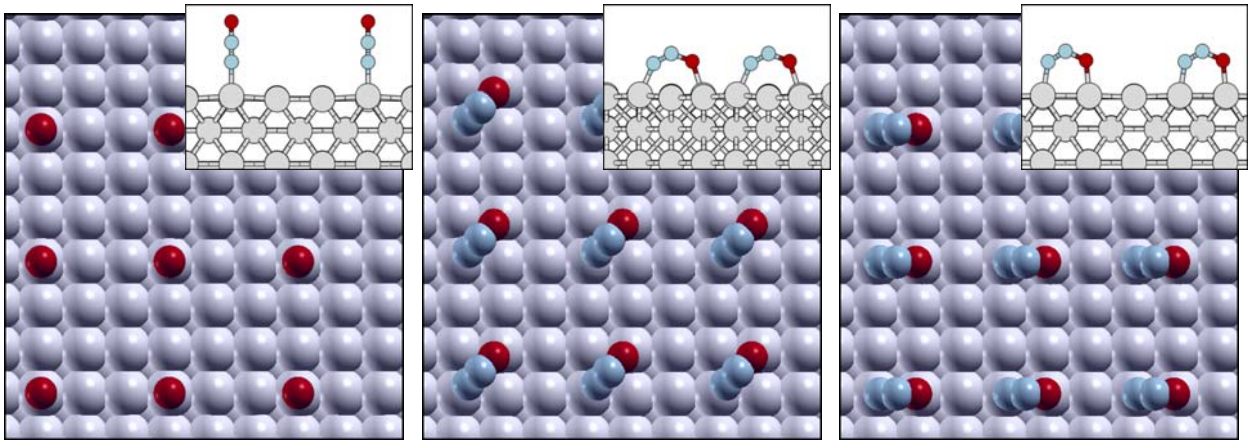

upright top	lying top along [001]	lying top along [011]
E_{ads} = 0.46 eV	E_{ads} = 0.40 eV	E_{ads} = 0.50 eV

Fig. 3 Mat